Investigation of the Cu^{II}/NCS^{-}/dpk Reaction System in CH_3OH [dpk = Di(2-pyridyl) Ketone]: Isolation, Structural Analysis and Magnetic Properties of a Dimer and a 1D Polymer with the Same Empirical Formula $[Cu(NCS)_2(dpk{\cdot}CH_3OH)]$

Zurine E. Serna,[a] Roberto Cortés,*[b] M. Karmele Urtiaga,[c] M. Gotzone Barandika,[b] Luis Lezama,[a] M. Isabel Arriortua,[c] and Teófilo Rojo*[a]

Keywords: N ligands / Copper / Coordination chemistry / EPR spectroscopy / Magnetic properties

Two polymorphous compounds with the general formula $[Cu(NCS)_2(dpk{\cdot}CH_3OH)]_n$ (dpk = di-2-pyridyl-ketone) have been synthesised and have been characterised both structurally and magnetically. The $dpk{\cdot}CH_3OH$ ligand is the result of the metal-promoted solvolysis of dpk in methanol and acts as a neutral donor. X-ray analysis carried out on single crystals for both compounds revealed that compound **1** is dimeric exhibiting double (*N*,*S*)-thiocyanate bridges, while compound **2** is 1D consisting of chains in which the metallic centres are connected through single *end-to-end* NCS^- groups. Magnetic susceptibility data showed that both compounds are antiferromagnetic, the values for the exchange constant *J* are –0.9 (**1**) and –0.3 cm^{-1} (**2**). The low values of *J* are consistent with the (N_{eq},S_{ax})-disposition of the thiocyanate bridges in the octahedral coordination sphere.

Introduction

High-dimensional arrangements exhibit potential applications in a great number of fields from heavy constructions to micro-circuitry.[1] Coordination polymers, in particular, have been the focus of attention of a great number of works devoted to the correlation between structural features and magnetic properties.[2] In this context, it is worth mentioning that the *N*,*N*′-type voluminous organic ligands have been extensively used, either as spacers or as coordination-site blockers.

Among the *N*,*N*′-donors, the di(2-pyridyl) ketone (dpk) ligand can be pointed out. This ligand exhibits certain singularities that explain its tendency to give rise to clusters[3] rather than infinite extended lattices when polynuclear systems are formed. The ligand dpk has three potential donor sites, however, when the ketocarbonyl group of dpk undergoes metal-promoted solvation (Scheme 1), four donor sites are exhibited. The resulting hydrated ($dpk{\cdot}H_2O$) or "alcoholated" (dpk·ROH) derivative can chelate either in a protonated or deprotonated state. As a consequence, the coordination possibilities of dpk are multiple and have been widely reported in the literature.[3,4] For instance, Tsohos et al.[3d] have reported a nonanuclear Co^{II}-dpk compound that clearly illustrates the capabilities of dpk. In this nonamer, the hydrated dpk derivative acts as a tetradentate ligand that is bonded to five different atoms of cobalt. This concentration of metallic ions around an organic molecule is obviously due to the proximity of the four potential donor atoms.

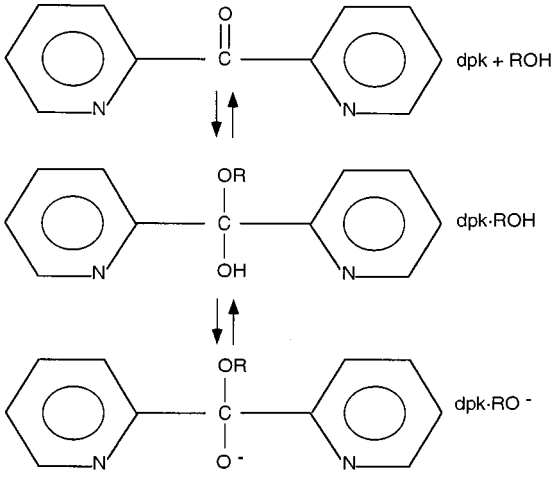

Scheme 1

The versatility of dpk could also be useful for the preparation of infinite arrays. To prevent cluster formation, pseudohalides could be used in combination with the organic ligand (as commonly carried out for other *N*,*N*′-

[a] Departamento de Química Inorgánica, Facultad de Ciencias, Universidad del País Vasco (UPV/EHU), Aptdo. 644, 48080 Bilbao, Spain
E-mail: QIPROAPT@lg.ehu.es
[b] Departamento de Química Inorgánica, Facultad de Farmacia, Universidad del País Vasco (UPV/EHU), Aptdo. 450, 01080 Vitoria, Spain
E-mail: QIPCOMOR@lg.ehu.es
[c] Departamento de Mineralogía y Petrología, Facultad de Ciencias, Universidad del País Vasco (UPV/EHU), Aptdo. 644, 48080 Bilbao, Spain

  1434–1948/01/0303–0865 $ 17.50+.50/0

groups). With this aim, we have been working on Ni^{II}-dpk-L systems (L = N_3, NCO, NCS). However, our first results have confirmed the tendency of dpk to concentrate metallic ions around it, through the characterisation of some tetramers.[4j,4k]

In order to explore the possibility of obtaining infinite polynuclear systems with other metals, this work was focused on Cu^{II}-systems. For this metallic cation a 1D arrangement has been synthesised. In particular, the results herein reported concern the magnetic and structural characterisation of two polymorphs with the general formula $[Cu(NCS)_2(dpk{\cdot}CH_3OH)]_n$. Compound **1** is a dimer exhibiting double (*N*,*S*)-thiocyanate bridges, while compound **2** consists of chains in which the metallic centres are connected through single *end-to-end* NCS^- groups. In both cases, the alcoholated dpk-derivative, dpk·CH_3OH, acts as a tridentate ligand and bonds to a single copper atom.

Results and Discussion

Structural Analysis

The structures of **1** and **2** are shown in Figure 1 and Figure 2, respectively. As observed, compound **1** consists of Cu^{II} dimers in which the metallic cations are connected through di-μ-(1,3)-NCS bridges, while compound **2** consists of chains in which the metallic cations are connected through single *end-to-end* thiocyanate bridges. The intermetallic distances through the thiocyanate bridges are 5.393 (**1**) and 5.994 (**2**) Å.

The octahedral coordination sphere around the Cu^{II} cations is similar for both polymorphous compounds. Thus, in both compounds the axial positions are occupied by S and O atoms: S1 corresponding to a bridging thiocyanate group and O1 belonging to the dpk·CH_3OH group. The formation of the dpk·CH_3OH is as a result of the solvolysis of the original dpk in methanol. At the equatorial positions, four N-atoms can be found, N3 and N4 atoms corresponding to a bridging and a terminal thiocyanate, respectively, and N1 and N2 belonging to the organic ligand. Thus, the main difference between **1** and **2** lies in the fact that in **1** each copper centre is connected to another copper centre through the S1 and N3 atoms, while in **2** each copper centre is connected to two other copper centres, one through the S1 atom and the other through the N3 atom. In this way, Cu^{II}-chains extend along the y direction for **2**.

The coordination sphere around the Cu^{II} cations in both compounds is noticeably distorted. This distortion can be attributed to the *N*,*O*,*N*′-terdentate coordination of dpk·CH_3OH and the long Cu−S distances. As can be seen in Table 1, the axial distances [Cu−S1 = 2.852(2) Å and Cu−O1 = 2.487(4) Å for **1**, and Cu−S1 = 2.837(1) Å and Cu−O1 = 2.503(2) Å for **2**] are remarkably higher than the equatorial ones [Cu−N average distances are 1.987 (**1**) and 1.991(**2**) Å]. The terdentate chelation of dpk·CH_3OH results in an angle of 109.8° (**1**) and 115.5° (**2**) between both pyridyl rings, as well as in important deviations from the ideal octahedral angles.

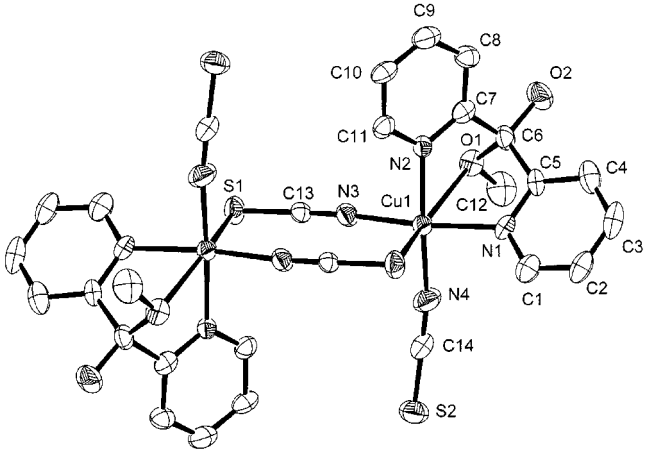

Figure 1. ORTEP view (50% probability) of the structure for compound **1** (H atoms are omitted for clarity)

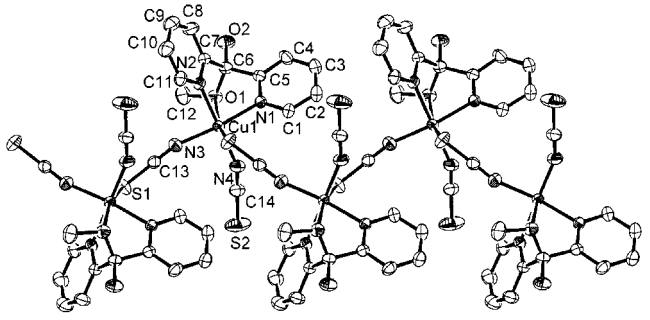

Figure 2. ORTEP view (50% probability) of the structure for compound **2** (H atoms are omitted for clarity)

Table 1. Selected bond lengths (Å) and angles (°) for compounds **1** and **2**

	1[a]	**2**[b]
Cu(1)−N(1)	2.026(5)	2.026(5)
Cu(1)−N(2)	2.022(4)	2.032(2)
Cu(1)−N(3)	1.945(5)	1.969(3)
Cu(1)−N(4)	1.956(5)	1.945(3)
Cu(1)−S(1i)	2.852(2)	2.837(1)
Cu(1)−O(1)	2.487(4)	2.503(2)
N(3)−C(13)	1.145(7)	1.145(4)
C(13)−S(1)	1.632(6)	1.637(3)
N(4)−C(14)	1.157(7)	1.143(4)
C(14)−S(2)	1.626(7)	1.620(3)
S(1i)−Cu(1)−O(1)	154.4(1)	162.78(5)
S(1i)−Cu(1)−N(1)	90.7(1)	96.76(7)
S(1i)−Cu(1)−N(2)	88.9(1)	91.90(7)
S(1i)−Cu(1)−N(3)	97.7(1)	93.45(9)
S(1i)−Cu(1)−N(4)	93.3(2)	92.3(1)
O(1)−Cu(1)−N(1)	72.1(1)	72.03(8)
O(1)−Cu(1)−N(2)	71.2(1)	74.62(8)
O(1)−Cu(1)−N(3)	98.2(2)	97.1(1)
O(1)−Cu(1)−N(4)	106.0(2)	101.2(1)
N(1)−Cu(1)−N(2)	87.1(2)	85.88(9)
N(3)−Cu(1)−N(2)	90.2(2)	90.0(1)
N(3)−Cu(1)−N(4)	92.0(2)	90.3(1)
N(4)−Cu(1)−N(1)	90.3(2)	93.1(1)
C(13)−N(3)−Cu(1)	171.9(5)	164.4(3)
N(3)−C(13)−S(1)	178.7(5)	179.6(3)
C(14)−N(4)−Cu(1)	167.0(6)	154.8(3)
N(4)−C(14)−S(2)	178.1(6)	179.1(3)

[a] *i* for this compound = 1 − *x*, −*y*, 1 − *z*. − [b] *i* for this compound = −*x*, 1/2 + *y*, 1/2 − *z*.

The structural features concerning the intermetallic connections are typical for thiocyanate bridges in octahedral systems.[5] Thus, both compounds exhibit the common $Cu-N_{eq}-C-S_{ax}-Cu$ coordination for the *end-to-end* thiocyanate bridge. On the other hand, the bridge-angles (N−C−S = 178.4°, C−S−Cu = 91.4°, S−Cu−N = 95.5° and Cu−N−C = 169.5° for **1**, and N−C−S = 179.3°, C−S−Cu = 91.4 °, S−Cu−N = 92.9° and Cu−N−C = 159.5° for **2**) show a slight deviation from the ideal ones.

It is worth mentioning that a great number of intermolecular and intramolecular H-bonds are present for both compounds (Table 2). As a result, the dimers (**1**) and the chains (**2**) are packed as displayed in Figure 3 and 4, respectively. As observed in Figure 3, there are magnetically nonequivalent ions which are related by the following operation of symmetry: x, $1/2 - y$, $1/2 + z$. The distance between these Cu atoms is 8.644(2) Å and the angle formed by the normals to their equatorial planes is 70.7(1)°. The presence of magnetically nonequivalent atoms in the unit cell will be used below in the EPR discussion. On the other hand, as seen in Figure 4, the packing of the chains in **2** allows π-π interactions between the pyridyl rings [inter-ring distance is 3.96(5) Å].

In summary, even if the dpk derivative in **2** acts as a tridentate ligand, the preparation of an extended dpk system has been possible as the organic ligand does not act as a bridging group but as a coordination-site blocker. In this sense, the role played by thiocyanate as the only intermetallic linker seems to be crucial to prevent the formation of clusters, as desired.

Table 2. Intermolecular[a] H-bond lengths (Å) and angles (°) for **1** and **2**

Compound 1

Donor−H	Donor···Acceptor	H.···Acceptor	Donor−H···.Acceptor
O2−H13	O2···S2(i)	H13···S2(i)	O2−H13···S2(i)
0.820(4)	3.330(4)	2.547(2)	160.4(3)
C8−H8	C8···N3(ii)	H8···N3(ii)	C8−H8···N3(ii)
0.930(6)	3.531(8)	2.912(5)	125.2(4)
(i) $2 - x$, $-y$, $2 - z$		(ii) x, $1/2 - y$, $1/2 + z$	

Compound 2

Donor−H	Donor···Acceptor	H···Acceptor	Donor−H···Acceptor
C8−H8	C8···O2(i)	H8···O2(i)	C8−H8···O2(i)
0.930(4)	3.489(5)	2.606(4)	158.7(2)
(i) $-x + 1$, $-y$, $-z$			

[a] The intramolecular ones can be found in the Supporting Information.

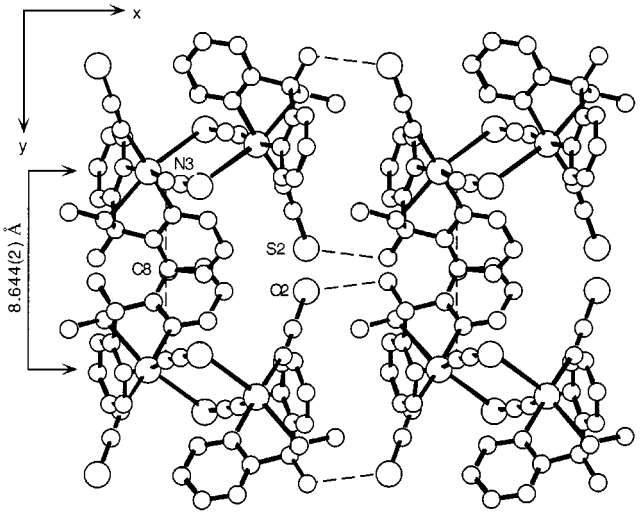

Figure 3. View of the packing of the dimers for **1** on the xy plane; discontinuous lines represent H-bonds (see Table 2); the magnetically nonequivalent atoms are located at 8.644(2) Å

IR Spectroscopy

A summary of the most important IR bands corresponding to compounds **1** and **2**, together with their tentative assignments[6] are given in Table 3. As can be seen, both compounds exhibit a split absorption at about 2100 cm^{-1} that corresponds to the asymmetric stretching mode of the C=N bond for the *N*,*S*-bonded thiocyanate.

In relation to the absorptions caused by the organic ligand, it is worth mentioning that the band at 1680 cm^{-1}, assigned to the C=O bond in conjugation with the pyridyl rings in dpk, is shifted to lower frequencies after solvolysis due to the presence of the C−O bond.[7] The bands assigned to the pyridyl ring stretching modes in **1** and **2** are also remarkably shifted, relative to the free dpk ligand, due to the loss of coplanarity between the pyridyl rings after rehybridisation from sp^2 to sp^3. The IR spectra also revealed the bands corresponding to the skeleton vibrations of the coordinated dpk·CH_3OH, which appear at slightly shifted frequencies relative to the free dpk.

EPR Spectroscopy

X- and Q-band powdered EPR spectra for **1** were recorded at room temp. down to 4.2 K. The spectra do not significantly change with temperature; a slight narrowing of the linewidth with decreasing temperature is observed. Q-band spectra, however, are better resolved than X-band ones. Figure 5 shows the Q-band spectrum for **1** at room temp. The signal seems to be rhombic, as is usually related to an exchange *g*-tensor. Additionally, there is a weak, broad signal at about 10750 G that must also be considered.

In order to interpret the spectrum in Figure 5 some structural features should be taken into account. The Cu^{II} octahedra in **1** are axially elongated suggesting that the molecular *g*-tensor is axial. However, it is also worth noting that compound **1** exhibits magnetically nonequivalent ions (Figure 3) that could involve interdimeric interactions. If the exchange interaction between nonequivalent centres were higher than the difference between the relative Zeeman energies, the EPR spectrum would not reveal the characteristics of the molecular *g*-tensor, but would show the ones corresponding to an average exchange *g*-tensor, g^{ex}. In that case, the components of the g^{ex} tensor could be expressed as a function of the components of the molecular *g*-tensor and the angles between them:[8] $(g_1^{ex})^2 = g_{\parallel}^2\cos^2\alpha + g_{\perp}^2\mathrm{sen}^2\alpha$ $(g_2^{ex})^2 = g_{\parallel}^2\mathrm{sen}^2\alpha + g_{\perp}^2\cos^2\alpha$ $g_3^{ex} = g_{\perp}$

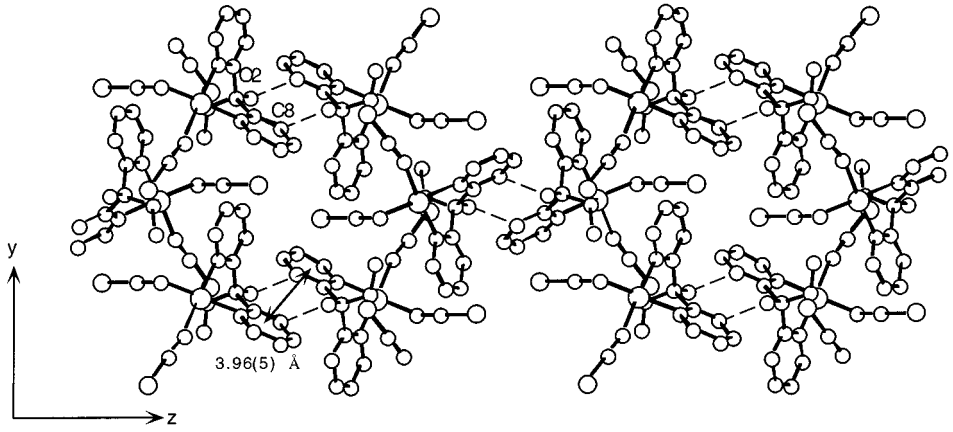

Figure 4. Packing of the dimers for **2** on the yz plane showing the H-bonds as discontinuous lines (see Table 2); the distance between parallel pyridyl rings is 3.96(5) Å

Table 3. Selected IR bands (cm^{-1}) for free dpk and the title compounds, together with their assignments

	free dpk[a]	Compound **1**	Compound **2**
Thiocyanate, ν(CN)	-	2121s, 2095s	2122s, 2074s
ν(CO)	1680s	1605	1597
Pyridyl ring stretching	1578s	1441	1381
Pyridyl ring breathing	998	1057	1057
Pyridyl C−H out of plane bending	753s, 742s	774	774
Pyridyl ring in plane vibration	662	673	650

[a] s: strong.

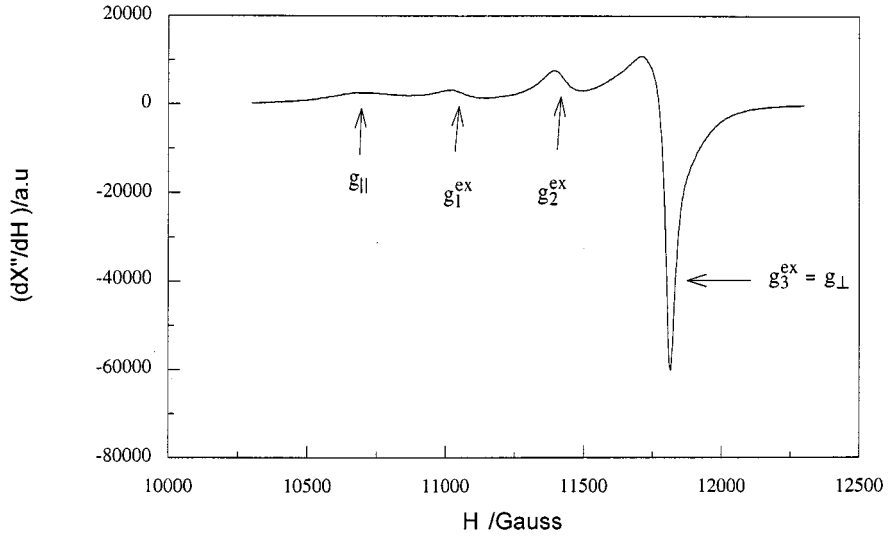

Figure 5. Q-band EPR powder spectrum at room temp. for **1**

where 2α is the angle formed by the magnetically non-equivalent chromophores; i.e. the canting angle between the normals to the equatorial planes of two interacting polyhedra [Equation (1)]:

$$\cos 2\alpha = \frac{g_1^{ex} - g_2^{ex}}{g_1^{ex} + g_2^{ex} - 2g_3^{ex}} \quad (1)$$

The observed values are $g_1^{ex} = 2.214$, $g_2^{ex} = 2.133$, $g_3^{ex} = 2.063$. Accordingly, $g_{\|} = 2.280$ and $g_{\perp} = 2.063$ have been calculated. The sequence $g_{\|} = 2.280 > g_{\perp} = 2.063 > 2.04$[8] agrees with the topology of the elongated [CuN_4SO] chromophores for **1**, as it corresponds to an ideal D_{4h} symmetry (d_x^2-$_y^2$ ground state). A calculated value of $2\alpha = 68°$ compares excellently with the crystallographic value of 70.7(1)°.

At this point, it is worth noting that the weak, broad signal on the spectrum that does not correspond to the rhombic tensor (ca. 10750 Gauss), but completely coincides with the $g_{\|}$ value deduced from g^{ex}. In other words, the spectrum seems to be the sum of two signals: those corresponding to the exchange and the molecular *g*-tensors. This unusual fact which has already been reported for two other

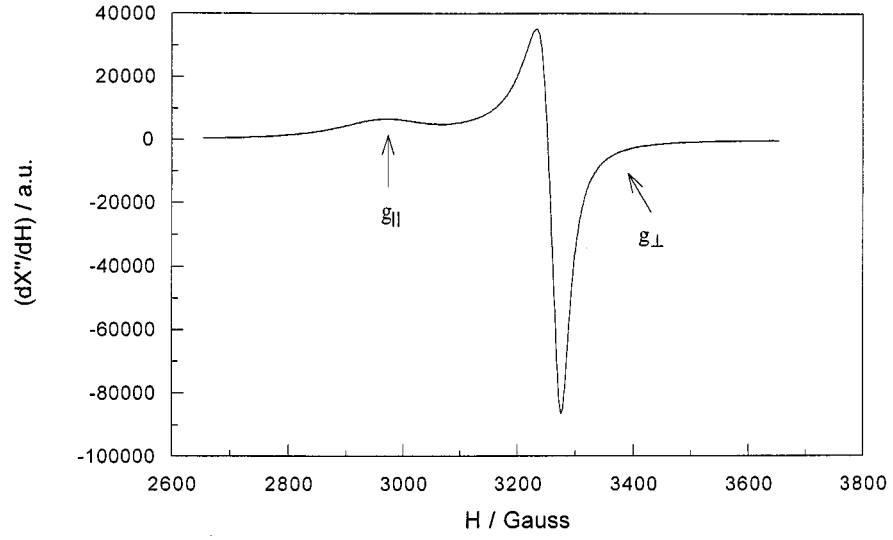

Figure 6. X-band EPR powder spectrum at room temp. for **2**

Cu^{II} compounds,[9] can only take place if the value of the exchange constant for the intermolecular coupling is similar to the Q-band energy-gap.

Figure 6 displays the X-band powdered EPR spectrum at room temp. for compound **2**. As observed, the signal is characteristic of an axial *g*-tensor with $g_{\|} = 2.258$ and $g_{\perp} = 2.052$. As for **1**, a slight narrowing of the linewidth is observed when the temperature is lowered from room temp. to 4.2 K. The *g* values account for a $d_{x^2-y^2}$ ground state, with an elongated octahedral copper(II) centre. They are in accordance with the $[CuN_4SO]$ chromophore corresponding to **2**.

Magnetic Properties

Compounds **1** and **2** were magnetically characterised through measurements of the thermal variation of the magnetic susceptibility, χ_m. Both polymorphous compounds exhibit similar magnetic behaviour. Thus, for both, χ_m continuously increases upon cooling (from 2.03×10^{-3} and 1.31×10^{-3} cm^3mol^{-1} at room temp. for **1** and **2**, respectively), the increase becoming exponential at temperatures tending to zero.

Figure 7 and 8 show the thermal variation of the $\chi_m T$ product and χ_m^{-1} for **1** and **2,** respectively. As can be seen, the $\chi_m T$ magnitude remains practically constant down to 25 K (**1**) and 50 K (**2**), temperatures below which the $\chi_m T$ values rapidly decrease towards zero. On the other hand, the Curie−Weiss law is followed over the whole measured temperature range in both cases. The calculated values of C_m and *g* (0.432 (**1**) and 0.429 (**2**) cm^3 K mol^{-1} and 2.146 (**1**) and 2.138 (**2**), respectively) are typical for an octahedrally-coordinated Cu^{II}.[10] The Weiss temperature, θ, has been observed to be −0.71 and −0.40 K, for **1** and **2**, respectively.

The above-mentioned aspects are indicative of the occurrence of antiferromagnetic exchange coupling which should take place through the thiocyanate intermetallic bridges. In order to evaluate the extension of these magnetic interactions, Equation (2) and (3) were used for **1** and **2**, respectively.

$$\chi_m = \frac{Ng^2\beta^2}{3kT}\frac{1}{1+\frac{exp(-2J/kT)}{3}} \quad (2)$$

$$\chi_m = \frac{Ng^2\beta^2}{kT}\frac{A+Bx+Cx^2}{1+Dx+Ex^2+Fx^3} \quad (3)$$

$A = 0.25,\quad B = 0.14995,\quad C = 0.30094,\quad D = 1.9862,\quad E = 0.68854,\quad F = 6.0626$

$x = J/kT$

where *N* and *k* are the Avogadro and Boltzmann constants, respectively, and β is the Bohr magneton.

The first of the expressions [Equation (2)][11] evaluates χ_m as a function of the exchange constant *J* for dimers with $S = 1/2$. The best fit parameters for **1** have been observed to be $J = -0.9$ cm^{-1} and $g = 2.145$. As observed in Figure 7, where the calculated $\chi_m T$ curve is displayed, there is an excellent agreement between both the theoretical and experimental data. On the other hand, the second expression [Equation (3)][12] accounts for the antiferromagnetic coupling for a Heisenberg chain with $S = 1/2$. Thus, the best fit parameters for **2** have been calculated to be $J = -0.3$ cm^{-1} and $g = 2.142$. As observed in Figure 8, the theoretical $\chi_m T$ curve reproduces the experimental data quite well.

Magnetic and Structural Correlations

Table 4 summarises the *J* values found in the literature for other (*N*,*S*)−NCS-bridged octahedral systems.[5,13] As observed, all but one exhibit low values for the magnetic

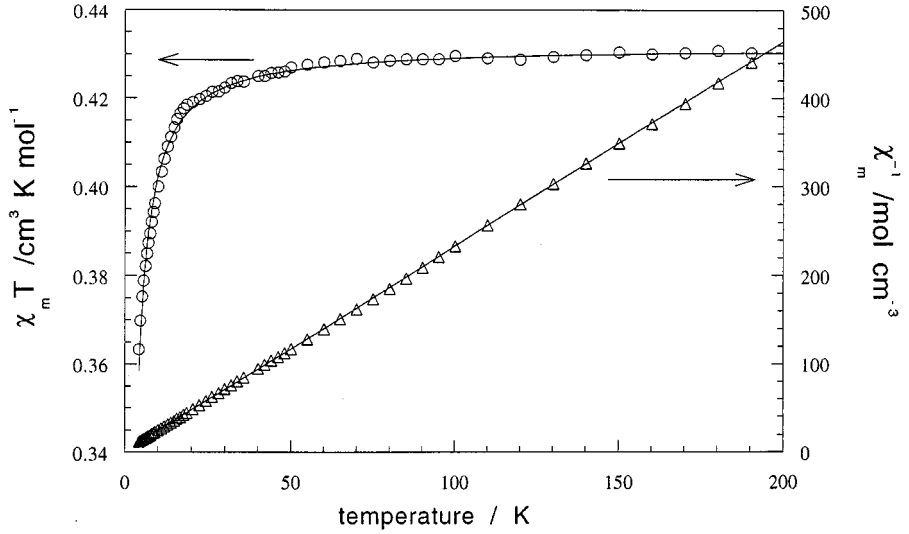

Figure 7. Thermal evolution of $\chi_m T$ and χ_m^{-1} for compound **1** and their corresponding theoretical curves

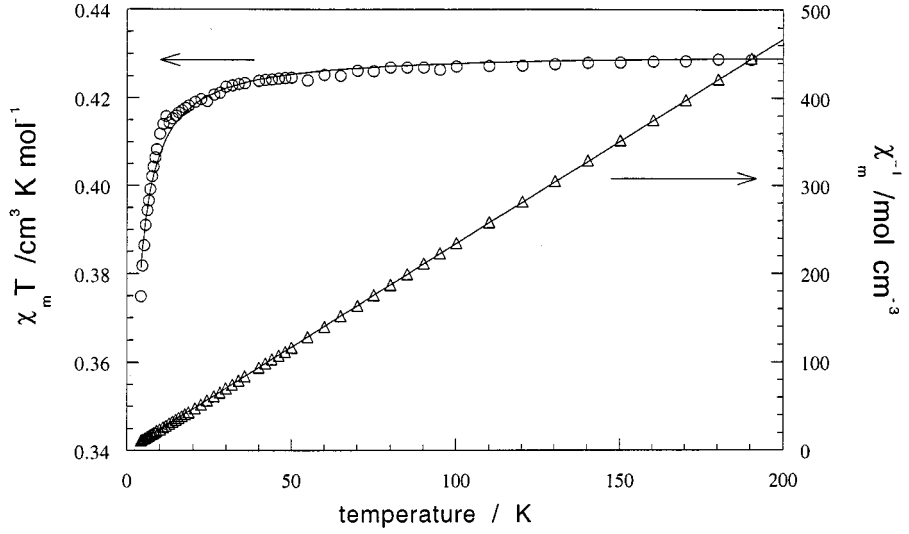

Figure 8. Thermal evolution of $\chi_m T$ and χ_m^{-1} for compound **2** and their corresponding theoretical curves

Table 4. Magnetic exchange constant J (cm^{-1}) for μ-(1,3)-NCS bridged Cu^{II} systems; N_e-S_a = N(equatorial)−S(axial) bridge; N_e-S_e = N(equatorial)−S(equatorial) bridge; Et_3dien = 1,4,7-triethyldiethylenetriamine; ept = *N*-(2-aminoethyl)-1,3-propanediamine; bheg = *N*,*N*-bis(2-hydroxyethyl)glycinato; bmp = 2,2′-bipyrimidine; Hmtpo = 4*H*,7*H*,5-methyl-7-oxo[1,2,4]triazolo[1,5-*a*]-pyrimidine; neg = negligible

Compound	Bridging mode	J	Reference
$[Cu(bpm)(NCS)_2]_n$	N_e-S_a	−0.6	[5a]
$[Cu(bheg)(NCS)]_n$	N_e-S_a	neg	[5b]
$[Cu_2(NCS)_2(Et_3dien)_2](ClO_4)_2$	N_e-S_a	+7.7	[5c]
$[Cu_2(NCS)_2(ept)_2](ClO_4)_2$	N_e-S_a	+1.3	[5c]
$[Cu(4\text{-bromopyridine})_2(NCS)_2]_n$	N_e-S_a	−	[5d]
1	N_e-S_a	−0.9	this work
2	N_e-S_a	−0.3	this work
$\{[Cu(NCS)_2(Hmtpo)\text{-}(H_2O)]_2\}_n$	N_e-S_a $+N_e-S_e$	−148	[13]

exchange constant. It is worth noting that the common feature for the majority is the $N_{eq}-S_{ax}$ disposition of the bridge, while for the strongly antiferromagnetic compound[13] the "rare" $N_{eq}-S_{eq}$ bridge-mode can also be found. As discussed below this is in total agreement with the theoretical predictions.

On theoretical bases,[14] the $N_{eq}-S_{ax}$ disposition leads to the accidental orthogonality of the MO arising from the e_g metallic orbitals, minimising the antiferromagnetic component of the global J constant (as experimentally confirmed for octahedral systems). Therefore, the fact that the strongly antiferromagnetic compound in Table 4 cannot be described by this disposition confirms this theoretical analysis (which is obviously valid for both single and double *end-to-end* thiocyanate bridges).

Conclusions

The use of the pseudohalide thiocyanate in combination with the blocking ligand dpk has led to the preparation of two polymorphous Cu^{II}-compounds: a 1D polymer and a

Table 5. Crystal data and structure refinements for **1** and **2**

Compound	**1**	**2**
Formula	$C_{14}H_{12}CuN_4O_2S_2$	$C_{14}H_{12}CuN_4O_2S_2$
M_w	395.95	395.95
Crystal system	Monoclinic	Monoclinic
Space group	$P2_1/c$	$P2_1/c$
a [Å]	11.673(2)	9.080(1)
b [Å]	17.215(3)	8.942(2)
c [Å]	8.295(2)	20.653(4)
β [°]	108.13(2)	103.54(2)
V [Å^3]	1584.1(5)	1630.3(5)
Z	4	4
$\rho_{cald.}$ [g.cm^{-3}]	1.660	1.613
μ (Mo-K_α) [cm^{-1}]	16.55	16.0
T [K]	20	20
λ (Mo-K_α) [Å]	0.71070	0.71070
Reflections collected	4878	5033
Unique data measured	4588	4746
Observed data with $I \geq 2.5\sigma(I)$	1771	3036
Number of parameters refined	211	211
R[a]	0.0627	0.0392
wR^2[b]	0.0954	0.1054

[a] $R(F_o) = (\Sigma||F_o| - |F_c||)/(\Sigma|F_o|)$. – [b] $wR(F_o^2) = \{\Sigma[w(F_o^2 - F_c^2)^2]/\Sigma[w(F_o^2)^2]\}^{1/2}$.

dimer. In both cases, the metallic cations are coordinated in a similar way to dpk·CH_3OH as well as to terminal and *end-to-end* thiocyanate groups. The dpk·CH_3OH is the result of the metal-promoted solvolysis of dpk in methanol. Both compounds are weakly antiferromagnetic as expected for the (N_{eq},S_{ax})-type intermetallic bridges.

Experimental Section

Synthesis

The synthesis of the title compounds was carried out by mixing an aqueous solution of $CuCl_2·2H_2O$ (0.5 mmol, 10 mL) with an aqueous solution of NaNCS (1 mmol, 10 mL). After stirring for one hour, a solution of dpk (15 mmol, 50 mL) in methanol was added. A green precipitate immediately appeared. Methanol was then added until this precipitate dissolved. The resulting solution was left to stand at room temperature. After several days, two types of green X-ray quality single crystals were obtained: (**1**) elongated prismatic crystals (yield 17%) and (**2**) regular prismatic crystals (yield 23%). Elemental analysis and ICP results were in good agreement with the $C_{14}H_{12}CuN_4O_2S_2$ stoichiometry for both compounds. – **1:** calcd. C 42.47, H 3.05, Cu 16.05, N 14.15, S 16.19; found C 42.5, H 3.1, Cu 15.9, N 14.2, S 16.1. – **2:** calcd. C 42.47, H 3.05, Cu 16.05, N 14.15, S 16.19; found C 42.4, H 3.0, Cu 16.0, N 14.1, S 16.1.

Physical Measurements

Microanalyses were performed with a LECO CHNS-932 analyser. Analytical measurements were carried out in an ARL 3410 + ICP with a Minitorch equipment. IR spectroscopy was performed on a Nicolet 520 FTIR spectrophotometer in the 400−4000 cm^{-1} region. EPR spectra were recorded on powdered samples at X- and Q-band frequencies, with a Bruker ESP300 spectrometer equipped with a standard OXFORD low-temperature device calibrated by the NMR probe for the magnetic field, the frequency measured by using a Hewlett−Packard 5352B microwave frequency computer. Magnetic susceptibilities of powdered samples were carried out in the temperature range 1.8−300 K (at a value of 1000 Gauss of the magnetic field) using a Quantum Design Squid MPM5−7 magnetometer, equipped with a helium continuous-flow cryostat. The experimental susceptibilities were corrected for the diamagnetism of the constituent atoms (Pascal tables).

Crystal Structure Determination

Single-crystal X-ray measurements for compounds **1** and **2** were carried out at room temperature on an Enraf−Nonius CAD-4 diffractometer with graphite-monochromated Mo-K_α radiation, operating in ω/2θ scanning mode using suitable crystals for data collection. Accurate lattice parameters were determined from least-squares refinement of 25 well-centred reflections. Intensity data were collected in the θ range 1−30°. During data collection, two standard reflections periodically observed showed no significant variation. Corrections for Lorentz and polarisation factors were applied to the intensity values.

The structures were solved by heavy-atom Patterson methods using the program SHELXS-97[15] and refined by a full-matrix least-squares procedure on F^2 using SHELXL-97.[16] Non-hydrogen atom scattering factors were taken from the International Tables of X-ray Crystallography.[17] In Table 5, crystallographic data and processing parameters for compounds **1** and **2** are shown.

Crystallographic data (excluding structure factors) for the structures reported in this paper have been deposited with the Cambridge Crystallographic Data Centre as supplementary publication nos. CCDC-143208 (**1**) and CCDC-143207 (**2**). Copies of the data can be obtained free of charge on application to The Director, CCDC, 12 Union Road, Cambridge CB2 1EZ UK [Fax: (internat.) +44-1223/336-033; E-mail: deposit@ccdc.cam.ac.uk].

Acknowledgments

This work has been carried out with the financial support of the Universidad del País Vasco/Euskal Herriko Unibertsitatea (Grant UPV 130310-EB201/1998), the Gobierno Vasco/Eusko Jaurlaritza (Project PI96/39) and the Ministerio de Educación y Cultura (Project PB97−0637). Z. E. S. also thanks the Ministerio de Educación y Ciencia for the grant AP96 20174323.

[1] [1a] G. R. Desiraju, in *Crystal Engineering: Design of Organic Solids*, Elsevier, Amsterdam, **1989**; *Angew. Chem. Int. Ed. Engl.* **1995**, *34*, 2311−2313. – [1b] R. Robin, B. F. Abrahams, R. R. Barten, R. W. Gable, B. F. Huskiness, J. Lieu, *Supramolecular Architecture*, ACS, Washington DC, **1992**, Ch. 19.M.

[2] M. Turnbull, T. Sugimoto, L. K. Thomson, *Molecule-Based Magnetic Materials*, American Chemical Society, Washington, DC, **1996**.

[3] [3a] V. Tangoulis, C. P. Raptopoulou, A. Terzis, S. Paschalidou, S. P. Perlepes, E. G. Bakalbassis, *Inorg. Chem.* **1997**, *36*, 3996−4006. − [3b] V. Tangoulis, C. P. Raptopoulou, S. Paschalidou, A. E. Tsohos, E. G. Bakalbassis, A. Terzis, S. P. Perlepes, *Inorg. Chem.* **1997**, *36*, 5270−5277. − [3c] V. Tangoulis, C. P. Raptopoulou, S. Paschalidou, E. G. Bakalbassis, S. P. Perlepes, A. Terzis, *Angew. Chem. Int. Ed. Engl.* **1997**, *36*, 1083−1085. − [3d] A. E. Tsohos, S. Dionyssopoulou, C. P. Raptopoulou, A. Terzis, E. G. Bakalbassis, S. P. Perlepes, *Angew. Chem. Int. Ed.* **1999**, *38*, 983−985.

[4] [4a] A. C. Deveson, S. L. Heath, C. J. Harding, A. K. Powell, *J. Chem. Soc., Dalton Trans.* **1996**, 3173−3178. − [4b] A. Basu, T. G. Kasar, N. Y. Sapre, *Inorg. Chem.* **1988**, *27*, 4539−4542. − [4c] A. N. Papadopoulos, V. Tangoulis, C. P. Raptopoulou, A. Terzis, D. P. Kessissoglou, *Inorg. Chem.* **1996**, *35*, 559−565. − [4d] M. L. Tong, H. K. Lee, S. L. Zheng, X. M. Chen, *Chem. Lett.* **1999**, 1087−1088. − [4e] O. S. Sommerer, W. P. Jensen, R. A. Jacobson, *Inorg. Chim. Acta* **1990**, *172*, 3−11. − [4f] G. Alonzo, N. Bertazzi, F. Maggio, F. Benetollo, G. Bombieri, *Polyhedron* **1996**, *15*, 4269−4273. − [4g] S. L. Wang, J. W. Richardson, S. J. Brigg, R. A. Jacobson, W. P. Jensen, *Inorg. Chim. Acta* **1986**, *111*, 67−72. − [4h] C. A. Kavounis, C. Tsiamis, C. J. Cardin, Y. Zubavichus, *Polyhedron* **1996**, *15*, 385−390. − [4i] Z. Serna, M. G. Barandika, R. Cortés, M. K. Urtiaga, M. I. Arriortua, *Polyhedron* **1998**, *18*, 249−255. − [4j] Z. E. Serna, M. G. Barandika, R. Cortés, M. K. Urtiaga, G. E. Barberis, T. Rojo, *J. Chem. Soc. Dalton Trans.* **2000**, 29−34. − [4k] Z. E. Serna, L. Lezama, , M. K. Urtiaga, M. I. Arriortua, M. G. Barandika, R. Cortés, T. Rojo, *Angew. Chem. Int. Ed.* **2000**, *39*, 344−347. − [4l] A. D. Q. Ferreira, A. Bino, D. Gibson, *Inorg. Chim. Acta* **1997**, *265*, 155−161. − [4m] S. O. Sommerer, B. L. Westcott, A. J. Jircitano, K. A. Abboud, *Acta Cryst.* **1996**, *C52*, 1426−1428. − [4n] S. R. Breeze, S. N. Wang, J. E. Greedan, N. P. Raju, *Inorg. Chem.* **1996**, *35*, 6944−6951. − [4o] M. A. S. Goher, F. A. Mautner, *Polyhedron* **2000**, *19*, 601−606.

[5] [5a] M. Julve, M. Verdaguer, G. DeMunno, J. A. Real, G. Bruno, *Inorg. Chem.* **1993**, *32*, 795−802. − [5b] H. Yamaguchi, Y. Inomata, T. Takeuchi, *Inorg. Chim. Acta* **1990**, *172*, 105−112. − [5c] R. Vicente, A. Escuer, E. Peñalba, X. Solans, M. Font-Bardía, *Inorg. Chim. Acta* **1997**, *255*, 7−12. − [5d] M. Kabesova, M. Dunaj-Jurco, J. Soldánová, *Inorg. Chim. Acta* **1987**, *130*, 105−111.

[6] K. Nakamoto, *Infrared Spectra of Inorganic and Coordination Compounds*, John Wiley & Sons: New York, **1997**.

[7] R. R. Osborne, W. R. Mc Whinnie, *J. Chem. Soc. A* **1967**, 2075−2096.

[8] B. Hathaway, D. E. Billing, *Coord. Chem. Rev.* **1970**, 143−163.

[9] [9a] W. Henke, S. Kremer, D. Reinen, *Inorg. Chem.* **1983**, *22*, 2858−2863. − [9b] T. Rojo, M. Insausti, L. Lezama, J. L. Pizarro, M. I. Arriortua, R. Calvo, *J. Chem. Soc., Faraday Trans.* **1995**, *91*, 423−429.

[10] F. E. Mabbs, D.J. Machin, *Magnetism and Transition Metal Complexes*, Chapman and Hall: London, **1973**.

[11] B. Bleany, K. D. Bowers, *Proc. R. Soc. London Ser. A* **1952**, *214*, 451−463.

[12] [12a] J. W. Hall, Ph. D. Université de Caroline Nord, (USA), **1977**. − [12b] W. E. Hatfield, *J. Appl. Phys.* **1981**, *52*, 1985−1992.

[13] J. A. R. Navarro, M. A. Romero, J. M. Salas, M. Quirós, E. R. T. Tiekink, *Inorg. Chem.* **1997**, *36*, 4988−4991.

[14] [14a] M. Kabesova, R. Boca, M. Melnik, D. Valigura, M. Dunaj-Jurco, *Coord. Chem. Rev.* **1995**, *140*, 112−118. − [14b] A. P. Ginsberg, R. L. Martin, R. W. Brookes, R. C. Sherwood, *Inorg. Chem.* **1972**, *11*, 2884−2889.

[15] G. M. Sheldrick, *SHELXS-97. Program for the Solution of Crystal Structures*, University of Göttingen, Germany, **1997**a.

[16] G. M. Sheldrick, *SHELXL-97. Program for the Refinement of Crystal Structures*, University of Göttingen, Germany, **1997**b.

[17] *International Tables for X-ray Crystallography, Vol. IV*, Kynoch Press, Birmingham, **1974**.

Received July 17, 2000
[I00277]